Supplementary Information

Both IRBIT and Long-IRBIT bind to and coordinately regulate Cl^-/HCO_3^- exchanger AE2 activity through modulating the lysosomal degradation of AE2

Ryo Itoh[a], Naoya Hatano[b], Momoko Murakami[a], Kosuke Mitsumori[a], Tomoka Wakagi[a], Yoshino Kanzaki[a], Hiroyuki Kojima[a], Katsuhiro Kawaai[c], Katsuhiko Mikoshiba[d], Koichi Hamada[a], and Akihiro Mizutani*[a]

[a]Department of Pharmacotherapeutics, Showa Pharmaceutical University, Machida, Tokyo 194-8543, Japan; [b]Division of Applied Cell Biology, Graduate School of Interdisciplinary Science and Engineering in Health Systems, Okayama University, Okayama 700-8530, Japan; [c]Laboratory of Cell and Tissue Biology, Keio University School of Medicine, Tokyo, 160-8582, Japan; Shanghai Institute for Advanced Immunochemical Studies, ShanghaiTech University, Shanghai, 201210, China
*Correspondence to mizutani@ac.shoyaku.ac.jp

Figure S1

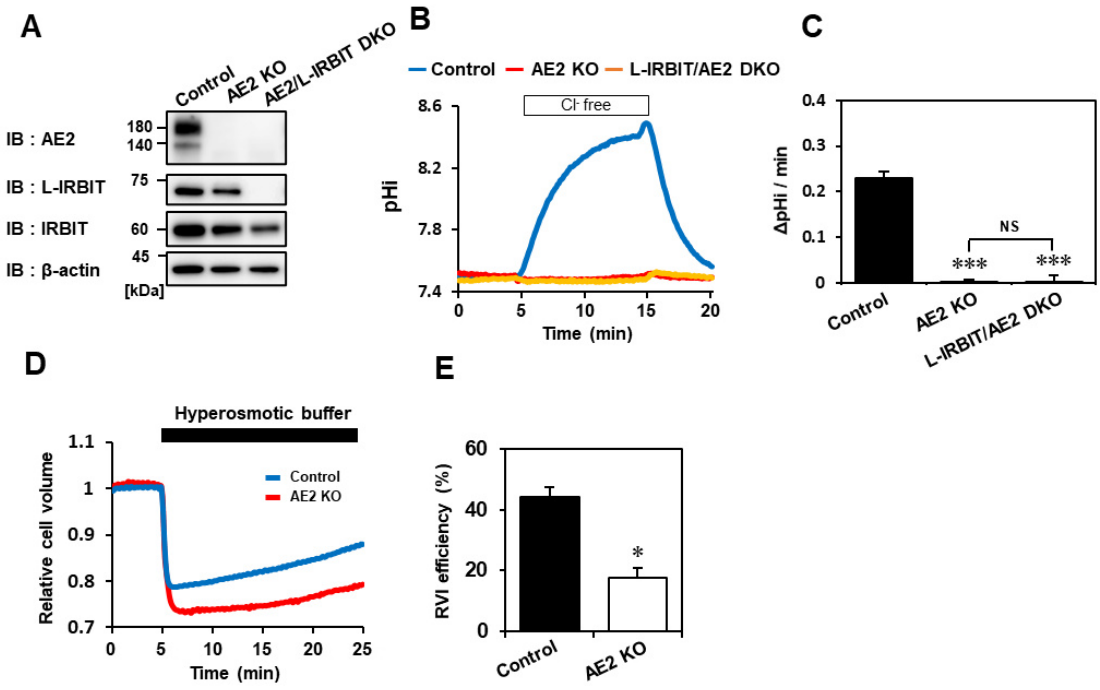

Figure S1. Cl^-/HCO_3^- anion exchange activity and cell volume recovery in AE2- or AE2/L-IRBIT double knockout cells. (A) AE2 and AE2/L-IRBIT double KO (DKO) cells were established by CRISPR/Cas9 strategy and their clones were verified for the expressions of IRBIT, Long-IRBIT and AE2 by immunoblot. (B) AE2 activity in AE2 KO cells or AE2/Long-IRBIT DKO cells was measured by intracellular pH changes (pHi) upon changing perfusion buffer from Cl^--containing to Cl^--free ringer buffers with SNARF1 pH sensitive dye. A representative plot of pHi changes obtained from control (blue), AE2 KO cells (red), and AE2/Long-IRBIT DKO cells (orange). (C) Average AE2 activity (ΔpHi/min) of each cell was 0.23 ± 0.2 (WT), 0.002 ± 0.003 (AE2 KO), and 0.001 ± 0.001 (L-IRBIT/AE2 DKO). N=3, ***P<0.001, N.S., no significance. (D) Cell volume recovery in AE2 KO cells was measured by fluorescence changes upon changing perfusion buffer from 300 mOsm buffer to 450 mOsm buffers with calcein-AM. A representative plot of fluorescence recovery rate as a relative cell volume from control (blue), AE2 KO clone1 (red). (E) RVI efficiency of each cells was 44.1 ± 3.3(WT), 17.6 ± 3.2 (AE2 KO). N=3, *P < 0.05.

Figure S2

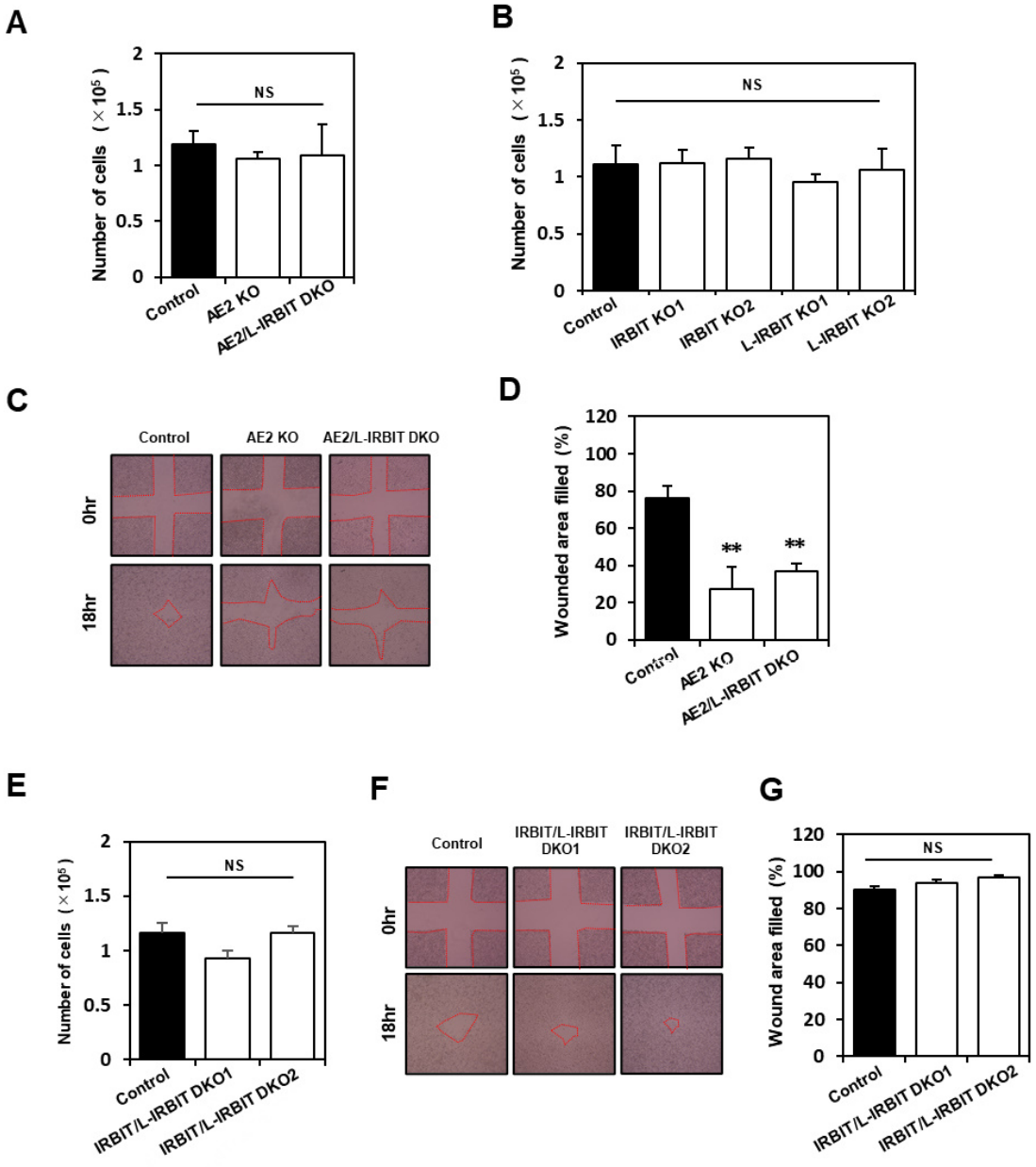

Figure S2. Cell growth and cell migration of IRBIT family- or AE2 knockout cells.

(A) The growth of control, AE2 KO and AE2/L-IRBIT double knockout (DKO) cells determined by direct cell count using a hemocytometer at 24 h after seeding. N=4, N.S., no significance. (B) The growth of control, IRBIT KO (IRBIT KO1, IRBIT KO2) and L-IRBIT KO (L-IRBIT KO1, L-IRBIT KO2) cells determined by direct cell count using a hemocytometer at 24 h. N=4, N.S., no significance. (C) The results of the wound healing assay were shown. Representative photomicrographs of the

wounded cell monolayer are shown. (D) Wound width was measured in 6 positions immediately after wounding and 18 h later in control, AE2 KO and AE2/Long-IRBIT DKO N=4, **P<0.01. (E) The growth of control, IRBIT/L-IRBIT DKO (IRBIT/L-IRBIT DKO1, IRBIT/L-IRBIT DKO2) cells determined by direct cell count using a hemocytometer at 24 h after seeding. N=4, N.S., no significance. (F) The results of the wound healing assay were shown. Representative photomicrographs of the wounded cell monolayer are shown. (G)Wound width was measured in 6 positions immediately after wounding and 18 h later in control and IRBIT/L-IRBIT DKO (IRBIT/L-IRBIT DKO1, IRBIT/L-IRBIT DKO2). N=4, N.S., no significance.

Figure S3

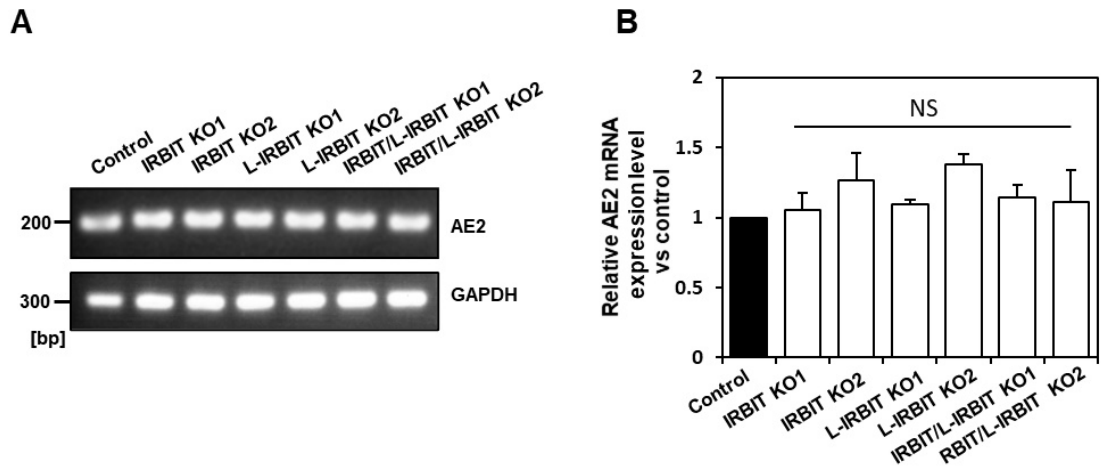

Figure S3. mRNA expression level of AE2 in IRBIT family knockout cells.

(A) mRNA expression level of AE2 and GAPDH were determined by RT-PCR using gene-specific primers. Representative data of amplified products by RT-PCR. (B) mRNA expression level of AE2 in each knockout cells was determined by qPCR using the delta Ct method ($2^{-\Delta\Delta Ct}$) with GAPDH as an internal control. N=4, N.S., no significance.

The images below are original ones before trimmed for a proper layout of each figure.

Figure 1A

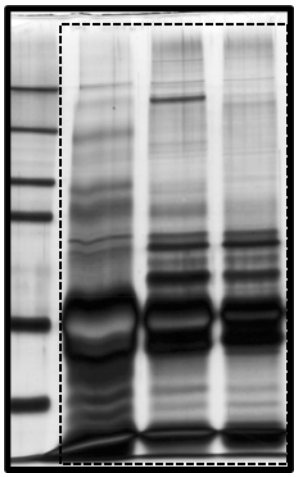

Figure 1B

IP : FLAG / IB : FLAG

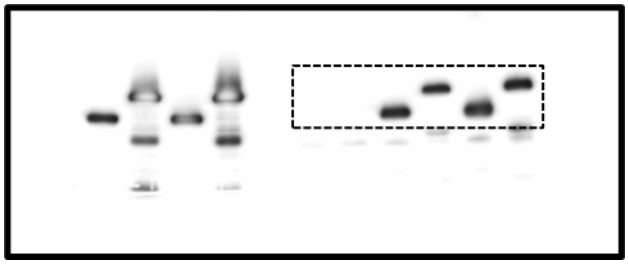

IP : HA / IB : HA

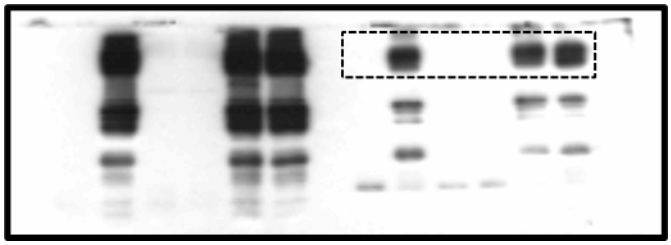

IP : FLAG / IB : HA

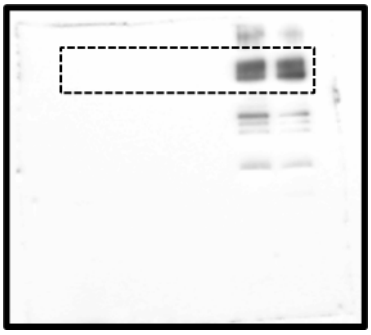

Input / IB : FLAG

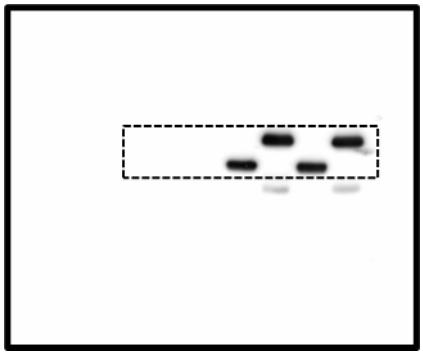

IP : HA / IB : FLAG

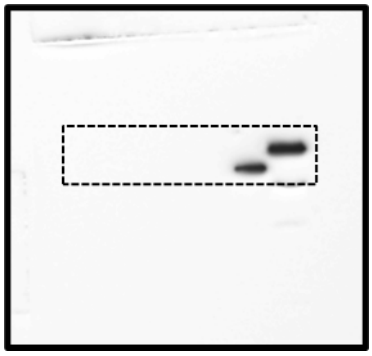

Input / IB : HA

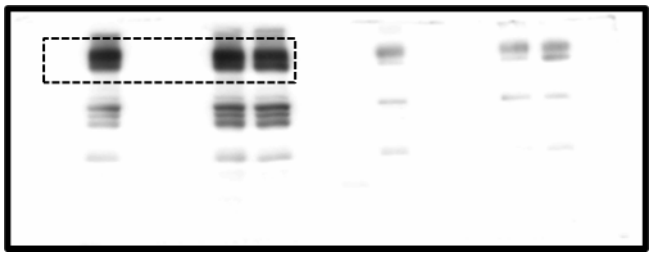

Figure 2A

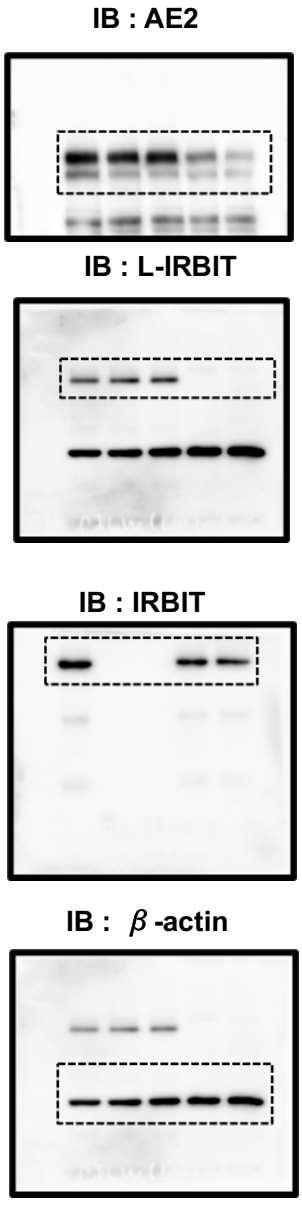

Figure 4B

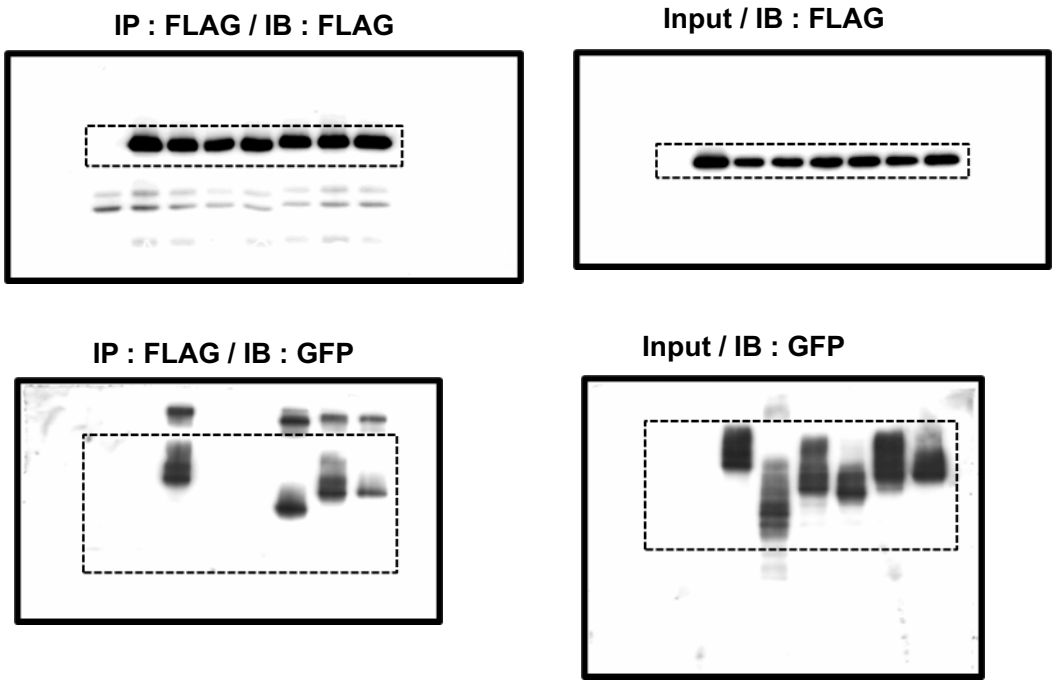

Figure 4C

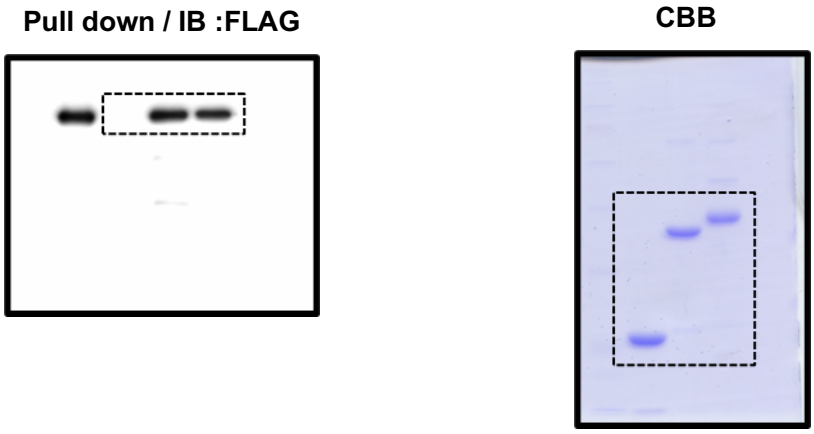

Figure 4D

Pull down / IB :FLAG

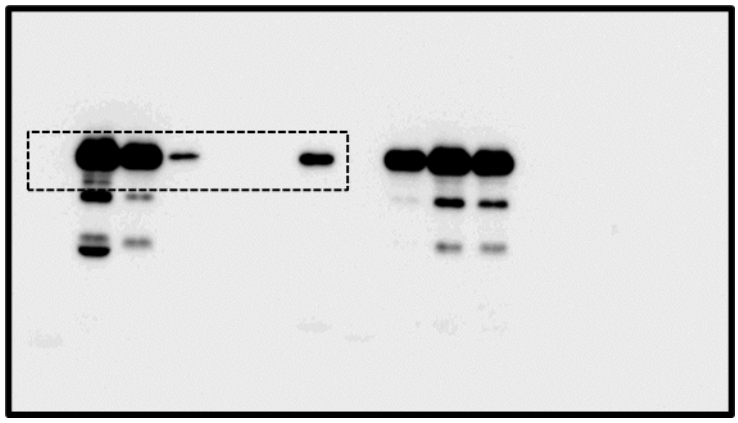

CBB

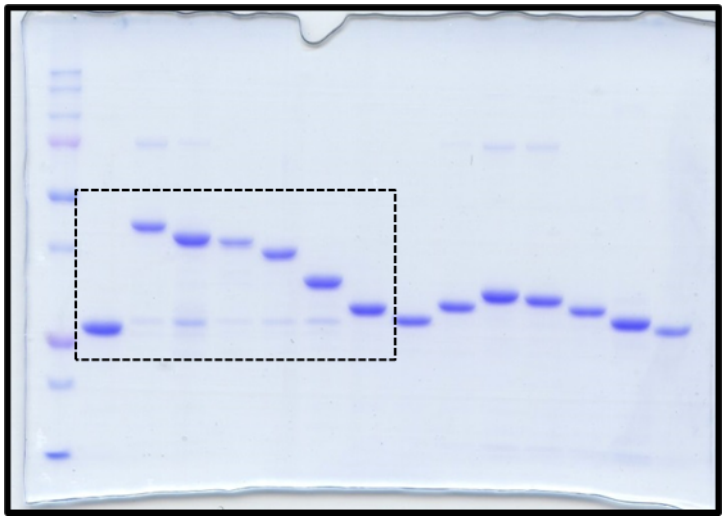

Pull down / IB :FLAG

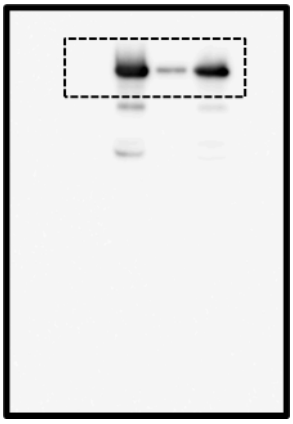

CBB

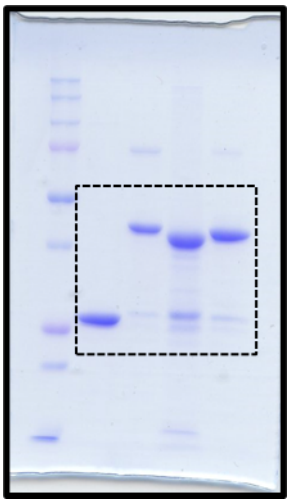

Figure 4E

IP : FLAG / IB : FLAG

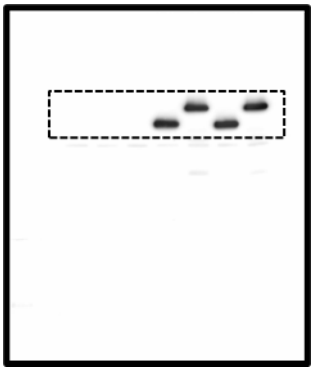

IP : HA / IB : HA

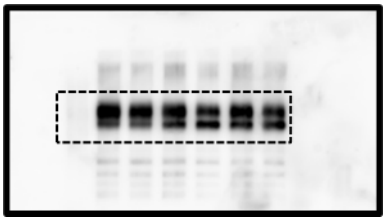

IP : FLAG / IB : HA

Input / IB : FLAG

IP : HA / IB : FLAG

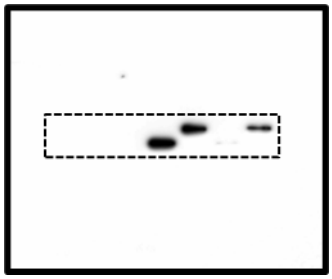

Input / IB : HA

Figure 5B

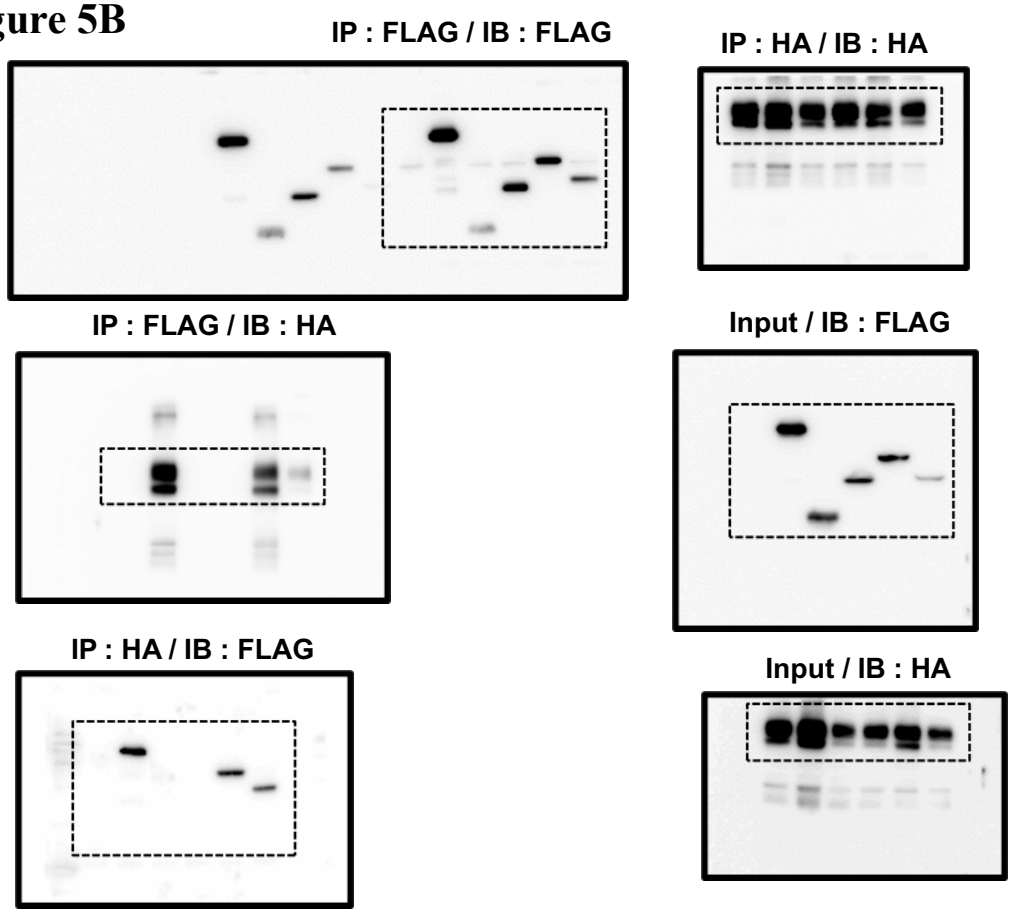
IP : FLAG / IB : FLAG
IP : HA / IB : HA
IP : FLAG / IB : HA
Input / IB : FLAG
IP : HA / IB : FLAG
Input / IB : HA

Figure 5C

Pull down / IB :MBP

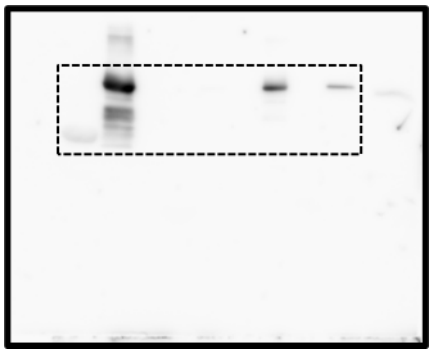

CBB

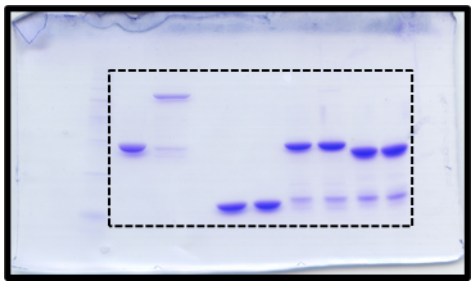

Figure 6B

IB : AE2

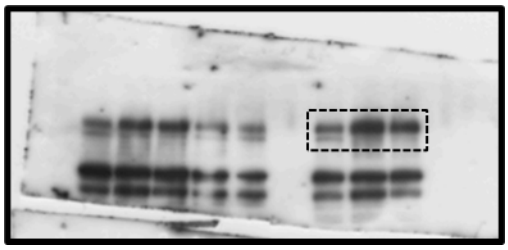

IB : L-IRBIT

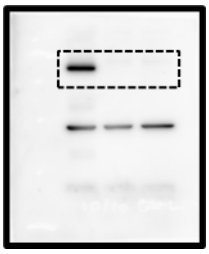

IB : IRBIT

IB : β -actin

Figure 7A

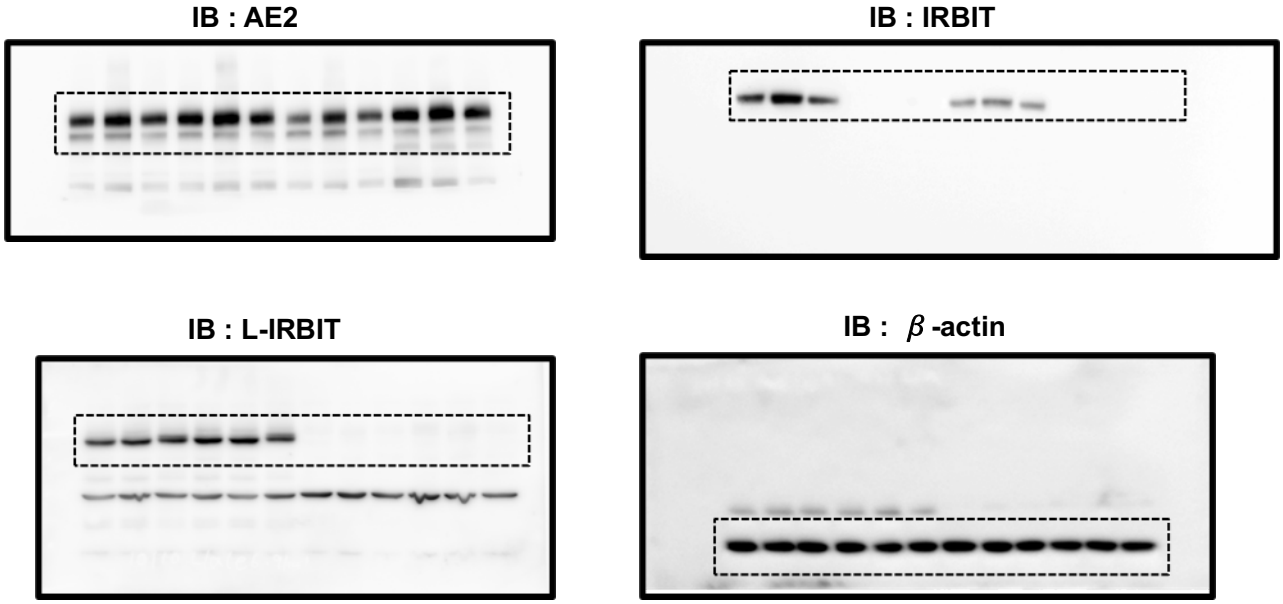

Figure 7B

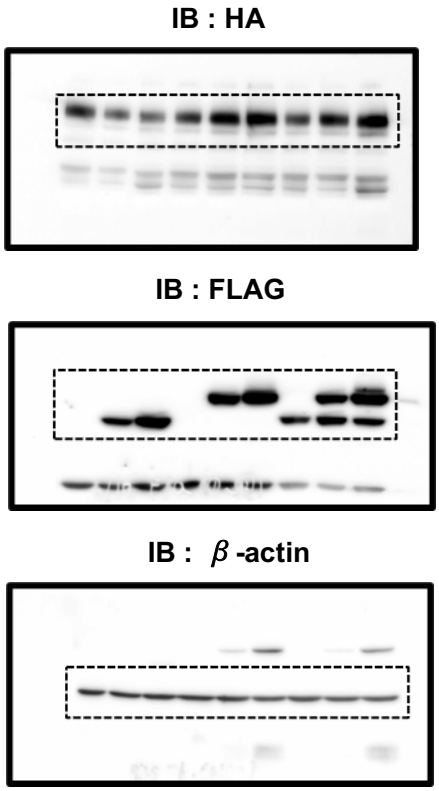

Figure 7C

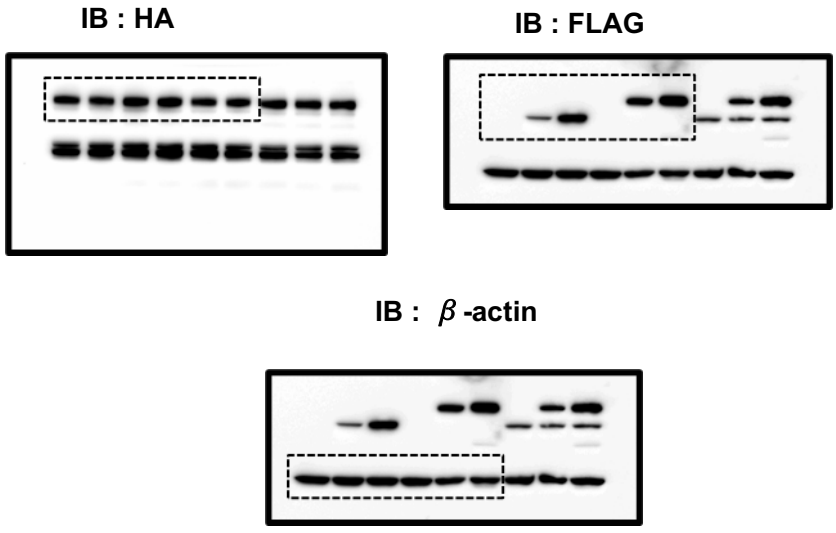

Figure 7D

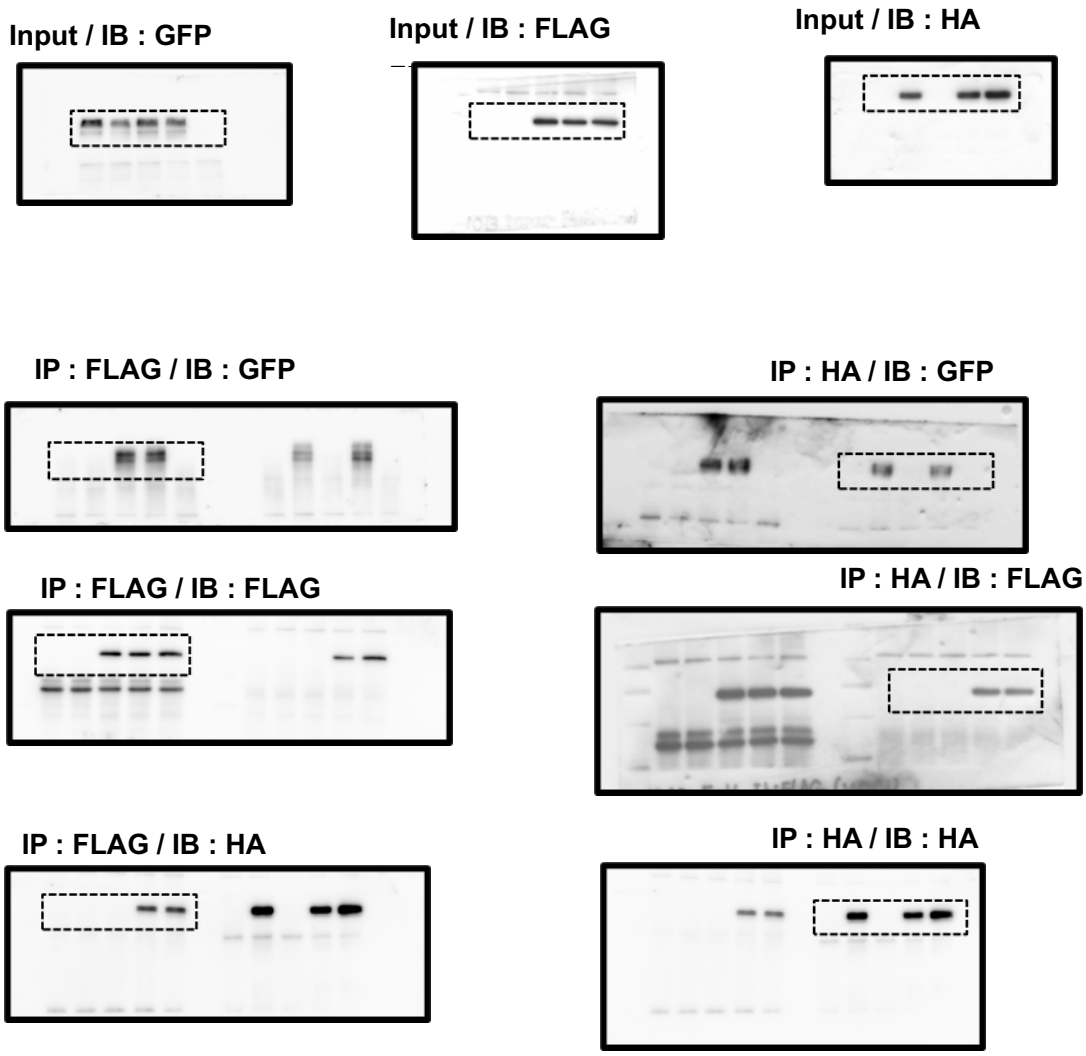
Input / IB : GFP
Input / IB : FLAG
Input / IB : HA
IP : FLAG / IB : GFP
IP : HA / IB : GFP
IP : FLAG / IB : FLAG
IP : HA / IB : FLAG
IP : FLAG / IB : HA
IP : HA / IB : HA

Figure S1A

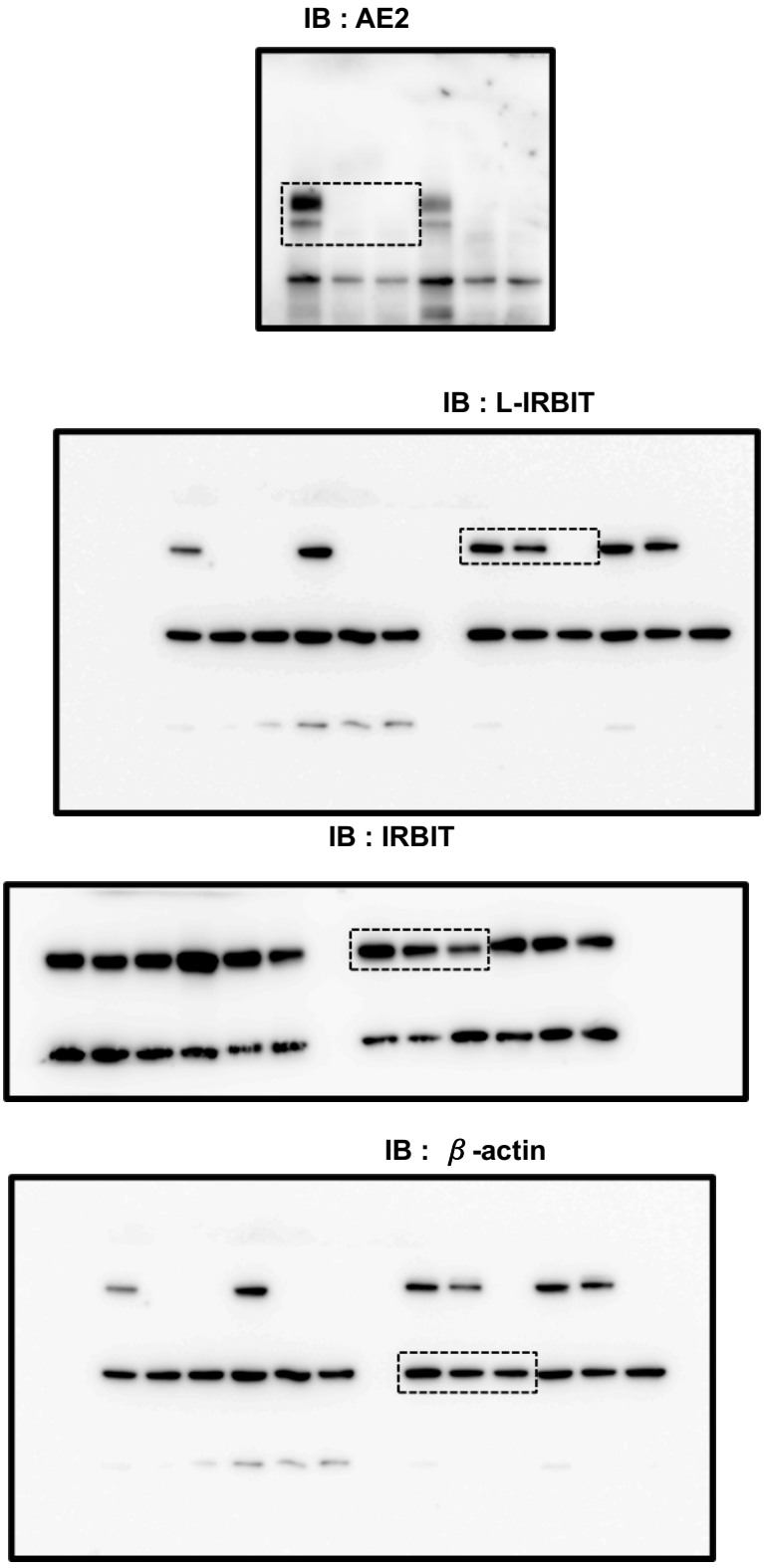

Figure S3A